A Synthetic Nervous System Controls a Biomechanical Model of *Aplysia* Feeding

Yanjun Li[1](✉), Victoria A. Webster-Wood[2], Jeffrey P. Gill[3], Gregory P. Sutton[4], Hillel J. Chiel[3], and Roger D. Quinn[1]

[1] Department of Mechanical and Aerospace Engineering, Case Western Reserve University, Cleveland, OH 44106-7222, USA
{yxl2259,rdq}@case.edu

[2] Department of Mechanical Engineering, Carnegie Mellon University, Pittsburgh, PA 15213, USA
vwebster@andrew.cmu.edu

[3] Department of Biology, Case Western Reserve University, Cleveland, OH 44106-7080, USA
{jeff.gill,hjc}@case.edu

[4] Department of Life Sciences, University of Lincoln, Lincoln, UK
gsutton@lincoln.ac.uk

Abstract. Building an accurate computational model can clarify the basis of feeding behaviors in *Aplysia californica*. We introduce a specific circuitry model that emphasizes feedback integration. The circuitry uses a Synthetic Nervous System, a biologically plausible neural model, with motor neurons and buccal ganglion interneurons organized into 9 subnetworks realizing functions essential to feeding control during the protraction and retraction phases of feeding. These subnetworks are combined with a cerebral ganglion layer that controls transitions between feeding behaviors. This Synthetic Nervous System is connected to a simplified biomechanical model of *Aplysia* and afferent pathways provide proprioceptive and exteroceptive feedback to the controller. The feedback allows the model to coordinate and control its behaviors in response to the external environment. We find that the model can qualitatively reproduce multifunctional feeding behaviors. The kinematic and dynamic responses of the model also share similar features with experimental data. The results suggest that this neuromechanical model has predictive ability and could be used for generating or testing hypotheses about *Aplysia* feeding control.

Keywords: Multifunctionality · Computational neuroscience · *Aplysia* · Control · Synthetic nervous systems

1 Introduction

As a basic motor control task, feeding is extensively studied in animals [1]. *Aplysia californica*, a species of sea slug, is a good model system for studying feeding for a number of reasons. It generates multifunctional feeding behaviors including biting, swallowing and rejection [2]. It uses a relatively small neural network to achieve complex

A. Hunt et al. (Eds.): Living Machines 2022, LNAI 13548, pp. 354–365, 2022.
https://doi.org/10.1007/978-3-031-20470-8_35

feeding control: its neural circuitry involved in feeding control contains about 2000 neurons. Additionally, the neurons can be uniquely identified across animals. With large and electrically compact soma, it is also possible to record or control neural activities through intracellular microelectrodes [3]. Fully understanding *Aplysia* feeding control could have significant impacts across various fields. For instance, it may be possible to discover how animals use a relatively small neural system to generate various behaviors adaptable to changes in environmental inputs and robust despite unpredictable variations in input, a critical capability for animals to survive in a changing environment [4]. Furthermore, the knowledge of *Aplysia* feeding control can be transferred to engineering, and could be used to design and control soft robotic graspers [5].

A computational model can enhance the understanding of *Aplysia* feeding control by providing a controlled platform to test hypotheses. Although the relatively small number and large size of neurons in *Aplysia*'s nervous system facilitate cell-level physiological studies, it is still difficult to experimentally test all neuronal biophysical properties and synaptic connections. For instance, both feedback pathways and pattern generators can be observed in the ganglia of *Aplysia* [2, 6], but the specific contributions of these mechanisms to feeding control remain unclear. Are pattern generators alone sufficient to generate multifunctional and robust feeding behaviors? Is the integration of feedback pathways into a small circuit sufficient for *Aplysia* feeding control? It is possible to address these questions using a computational model by running numerical simulations and comparing the results with animal data. Furthermore, predictions generated by models can lead to new hypotheses guiding future experiments [2].

Existing computational models of *Aplysia* feeding either lack essential neuromechanical elements or have limited biological plausibility. The model developed in [7] incorporates Hodgkin-Huxley-type neurons and complex synaptic dynamics to model key neurons in the buccal ganglion and CBI-2, a critical cerebral-buccal interneuron in the cerebral ganglion. It can generate ingestive-like motor patterns observed in isolated ganglia, but the lack of other cerebral-buccal interneurons (CBIs) prevents switching between different motor patterns. Moreover, the model does not consider the peripheral mechanics, so it cannot yet be used to study the effects of sensory feedback on neural activity and behavior. The complexity of Hodgkin-Huxley-type models also makes this approach challenging to scale to larger circuits. By employing a demand-driven approach, a neuromechanical model of *Aplysia* feeding was built in [2] using a Boolean neuron model. In this model, motor neurons and buccal interneurons are driven by proprioceptive feedback, and interneurons CBI-2, CBI-3, CBI-4 are responsible for coordinating biting, swallowing, and rejection based on exteroceptive feedback. The Boolean model can run several orders of magnitude faster than real-time, but its neurons only operate through logic operations, making the model less biologically plausible.

To meet the need for a scalable computational model to generate *Aplysia*-like kinematics, dynamics, and neural activities for multifunctional feeding behaviors, we developed an *Aplysia* neuromechanical model using a Synthetic Nervous Systems (SNSs) [8]. Like Hodgkin-Huxley-type neurons, the computational capability of an SNS comes from conductance-based mechanisms. SNSs can achieve a low computational complexity by locating all conductance within a single compartment and abstracting the spiking

activity of individual neurons using a rate model. Our neuromechanical model generalizes the model in [2] with the Boolean circuits replaced with SNS circuits. In particular, the motor neurons and buccal interneurons receiving proprioceptive feedback are organized in nine subnetworks to control *Aplysia* feeding behavior *in silico*. In addition, three cerebral-buccal interneurons (CBIs) coordinate feeding behaviors according to exteroceptive feedback. The CBIs generate behavioral transitions by flexibly coordinating different subnetworks. We find that the SNS neural circuitry can generate different feeding behaviors, including biting, swallowing, and rejection. Comparisons between the model output and experimental data provides further support for the model's plausibility. These results support the hypothesis that integrating feedback and a relatively small neural network can control a model of *Aplysia* biomechanics and generate multifunctional and robust feeding behaviors in simulation.

2 Methods

We developed an *Aplysia californica* feeding model extending a previous Boolean model of the *Aplysia* neural system [2] to a Synthetic Nervous System with additional neurons and more biologically plausible neural dynamics. The SNS model is organized into nine functional subnetworks and a cerebral ganglion layer coordinating the feeding behaviors based on known neural circuitry reported in the literature.

2.1 Biomechanical Model

The biomechanical model receives motor commands from the neural circuity model and returns proprioceptive feedback. This work adopts a simplified biomechanical model described in [2]. The peripheral mechanics represents a simplified *Aplysia* feeding system with two components connected by two translational degrees of freedom (DOFs) and actuated by four muscles. The components include the head and the grasper that are the main constituents of the feeding apparatus, also known as the buccal mass. Three muscle units, including the I2 protractor muscle, the I3 retractor muscle, and the hinge retractor muscle, actuate the head-grasper component. The remaining muscle unit, the I4 muscle, and the anterior portion of the I3 jaw muscle are responsible for grasper and jaw closure, respectively.

2.2 Synthetic Nervous System

The SNS is a rate model. A monotonically increasing activation function φ_i is used to represent the relationship between the activity y_i and the membrane potential U_i of the ith neuron $y_i = \varphi_i(U_i)$. A standard selection of φ_i is a piecewise linear function mapping the membrane potential to [0, 1]. Intuitively, y_i is an indicator of the temporal firing frequency of the corresponding neuron.

The dynamics of neurons in the SNS can be described as

$$I_{\text{cap},i} = I_{\text{leak},i} + I_{\text{ion},i} + I_{\text{syn},i} + I_{\text{app},i}, \tag{1}$$

where $I_{\mathrm{cap},i} = C_{\mathrm{m},i}\, \mathrm{d}U_i/\mathrm{d}t$ and $I_{\mathrm{leak},i} = G_{\mathrm{m},i}\,(E_{\mathrm{r},i} - U_i)$ are the capacitance current and leak current, respectively. $C_{\mathrm{m},i}$ is the membrane capacitance, $G_{\mathrm{m},i}$ is the membrane conductance, and $E_{\mathrm{r},i}$ is the neuron's resting potential. $I_{\mathrm{ion},i}$ represents the currents flowing through other voltage-gated ion channels responsible for strong nonlinear phenomena like plateau potentials and post-inhibitory rebound:

$$I_{\mathrm{ion},i} = \sum_{j=1}^{r} g_{p,j} A_j^{p_j} B_j (E_{p,j} - U_i). \tag{2}$$

For the jth ion channel, $g_{\mathrm{p},j}$ is the maximal conductance, $E_{\mathrm{p},j}$ is its reversal potential, and A_j and B_j are the activation and inactivation variables, respectively. p_j, the activation exponent, is an integer parameter typically from the set {1, 2, 3, 4}. The transient responses of A_j and B_j are modeled as

$$\begin{aligned} \frac{dA_j}{dt} &= \frac{A_{\infty,j} - A_j}{\tau_{A_j}} \\ \frac{dB_j}{dt} &= \frac{B_{\infty,j} - B_j}{\tau_{B_j}}, \end{aligned} \tag{3}$$

where $A(B)_{\infty,j}$ and $\tau_{\mathrm{A(B)}j}$ denote the membrane-potential-dependent steady-state and relaxation time of $A(B)$.

In Eq. (1), $I_{\mathrm{app},i}$ defines an optional applied external stimulus current. For example, feedback signals can be expressed as

$$I_{\mathrm{app}} = \sum_{l=1}^{m} \xi_l \max(\varepsilon_l (x_l - S_l)\sigma_l, 0), \tag{4}$$

with ξ_l and S_l representing the feedback gain and the threshold of the lth feedback input x_l. $\sigma_l \in$ {-1, 1} indicates the corresponding direction of the feedback, while $\varepsilon_l \in$ {-1, 1} is the feedback polarization (excitatory if $\varepsilon_l = 1$, inhibitory if $\varepsilon_l =$ -1). The remaining term, $I_{\mathrm{syn},i}$, encompasses currents through both chemical and electrical synapses:

$$I_{\mathrm{syn},i} = \sum_{j=1}^{n} G_{\mathrm{s},ij}\big(E_{\mathrm{s},ij} - U_i\big) + \sum_{k=1}^{m} G_{e,ik}\big(U_{\mathrm{pre},k} - U_i\big). \tag{5}$$

For the kth electrical synapse, $U_{\mathrm{pre},k}$ is the membrane potential of the presynaptic neuron and $G_{\mathrm{e},ik}$ is the electrotonic coupling conductance. For the jth chemical synapse, $E_{\mathrm{s},ij}$ is the reversal potential. In the SNS, the synaptic conductance $G_{\mathrm{s},ij}$ is written as $G_{\mathrm{s},ij} = g_{\mathrm{s},ij}\, r_{ij}$, where $g_{\mathrm{s},ij}$ is the maximal conductance. R_{ij}, the activation of the synapse in [0, 1], can be expressed as a cascade connection of two first-order linear systems:

$$\begin{aligned} \frac{ds_{ij}}{dt} &= \frac{y_{\mathrm{pre},j} - s_{ij}}{\tau_{\mathrm{syn},ij1}} \\ \frac{dr_{ij}}{dt} &= \frac{s_{ij} - r_{ij}}{\tau_{\mathrm{syn},ij2}} \end{aligned}. \tag{6}$$

In the above synaptic dynamics, $y_{\mathrm{pre},j}$ is the activity of the jth presynaptic neuron, while s_{ij} represents the activation of presynaptic transmitter release of the jth synapse. $\tau_{\mathrm{syn},ij1}$ and $\tau_{\mathrm{syn},ij2}$ are two characteristic activation time constants.

2.3 Neural Control Circuitry

Using the SNS framework, we developed a neural circuitry model of *Aplysia* feeding control based on known synaptic connections while taking into account the feedback signals from the peripheral biomechanics (Fig. 1).

Motor Control Layer. The motor control layer consists of 5 known motor neurons innervating key musculature: B31 innervates the I2 Protractor muscle for protracting the grasper [9]; B6 innervates the I3 retractor muscle for retracting the grasper [10]; B8 innervates the I4 muscle for closing the grasper [10]; b38 innervates the anterior portion of the I3 muscle for pinching the jaws to hold onto food during the protraction phase of swallowing [11]; B7 innervates the hinge muscle for facilitating initial retraction [12]. Activations of the five motor neurons are mediated by the higher buccal interneuron layer and sensory feedback (B38 and B7 receive proprioceptive feedback on the position of the grasper within the head, x_{gh} [2]).

Buccal Ganglion Layer. IN the buccal ganglion layer model, we organized nine buccal interneurons into five subnetworks (B63/B31, B64/B52, B34/B40, B65/B30, B20/B4) based on their known functional roles in biting, swallowing, or rejection (Fig. 2). A subnetwork can accomplish its function by stimulating a specific set of motor neurons. To coordinate the behaviors, subnetworks receive commands from the higher layer, while some buccal interneurons also receive proprioceptive feedback on the grasper position, x_{gh}. In addition, activation of a subnetwork can modulate activations of other subnetworks to achieve appropriate functional timing.

Subnetwork B63/B31 (Fig. 2A) realizes grasper protraction through strong excitatory synaptic connections between B63 and motor neuron B31 [13]. Because B63 and B31 can be viewed as a single functional unit [14], we assign motor neuron B31 and interneuron B63 to the same subnetwork. In contrast, subnetwork B64/B52 (Fig. 2A) enables grasper retraction by a monosynaptic connection between B64 and the motor neuron B6 [15]. Due to the intrinsic slowly activating sodium channel and the slowly inactivating potassium channel, B64 can spontaneously generate a plateau potential some time after its activation [7]. Proprioceptive feedback to B64 can extend the duration of retraction, enabling feeding to adapt to external load [2]. B52 can demonstrate a post-inhibitory rebound (PIR) phenomenon due to a low threshold sodium channel [6]. PIR, together with the mutual inhibitory connections, ensures the termination of the retraction phase. The transition from the protraction phase to the retraction phase is realized by a slow excitatory synapse from B63 to B64 [7].

Subnetwork B34/B40 (Fig. 2B) and B65/B30 (Fig. 2C) are responsible for mediating variations in protraction durations and closing the grasper during the retraction phase. Their activation is in phase with protraction since both subnetworks are driven by B63/B31 and inhibited by B64 [16]. B34 and B40 make monosynaptic inhibitory connections with B64 [7], postponing the onset of B64 and promoting a longer protraction duration [17]. In contrast, B65 and B30 make fast inhibitory and slow excitatory connections with B64 [16], thus activating an earlier plateau potential in B64 and promoting a shorter protraction duration [17]. In addition, both B40 and B30 promote grasper closure during the retraction phase by slow excitatory synapses to B8 [16].

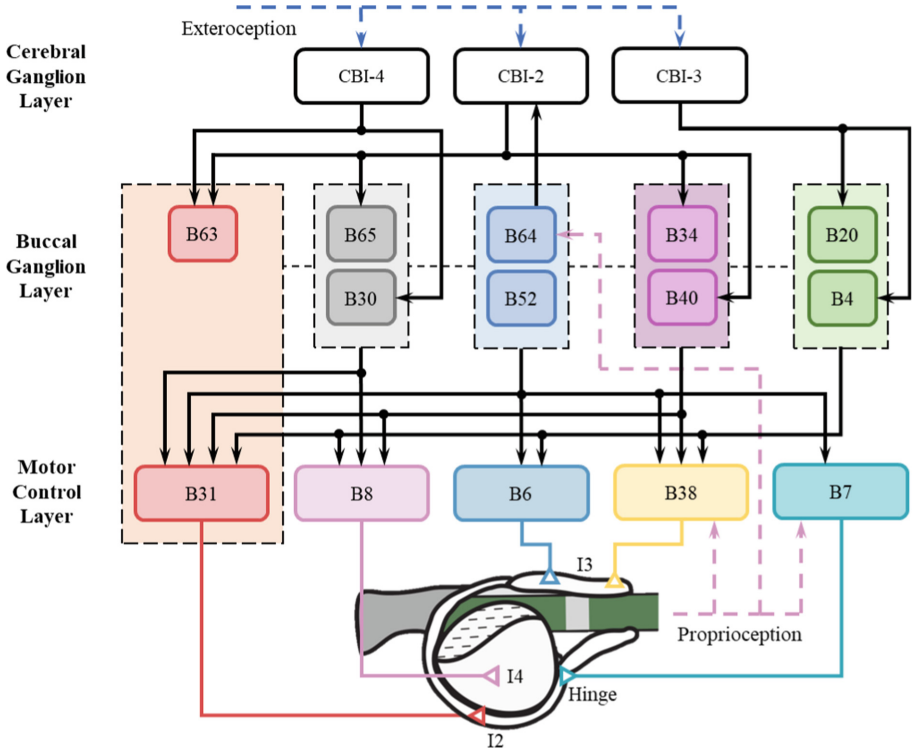

Fig. 1. Schematic of the neural circuitry model. In the motor control layer and buccal ganglion layer, we divided the neurons into nine subnetworks according to their functions. Neurons in the same subnetwork are indicated by the same color. The cerebral ganglion layer contains cerebral interneurons for behavior switching and coordination. Cross-layer synaptic connections are shown as bold black arrows. Dashed black lines represent intra-layer connections. Sensory signals, including proprioceptive and exteroceptive feedback, may be provided by additional sensory neurons or interneurons in the neural circuitry of the animal.

The last subnetwork modeled in this layer, B20/B4 (Fig. 2D), triggers grasper closure during the protraction phase and grasper relaxation during the retraction phase. B20 is excited by other protraction interneurons, indicating that it is activated in this phase [18]. Therefore, the excitatory synapse from B20 to B8 makes the grasper close during protraction. In addition, through the inhibitory synapse to B8, the hyperpolarization elicited by B4 can overcome the excitation produced by B40 or B30 during retraction.

Cerebral Ganglion Layer. The cerebral ganglion layer contains command-like neurons whose activation patterns encode which feeding behavior to generate. In this layer, the model incorporates the three critical cerebral-buccal interneurons, namely CBI-2, CBI-3, and CBI-4. CBI-3 strongly inhibits the B20/B4 subnetwork [18]. Thus, its activation determines the timing of grasper closure and differentiates between ingestive and egestive behaviors. CBI-2 and CBI-4 play a similar role in the rejection because they activate the protraction phase by exciting B63. However, their activations have different

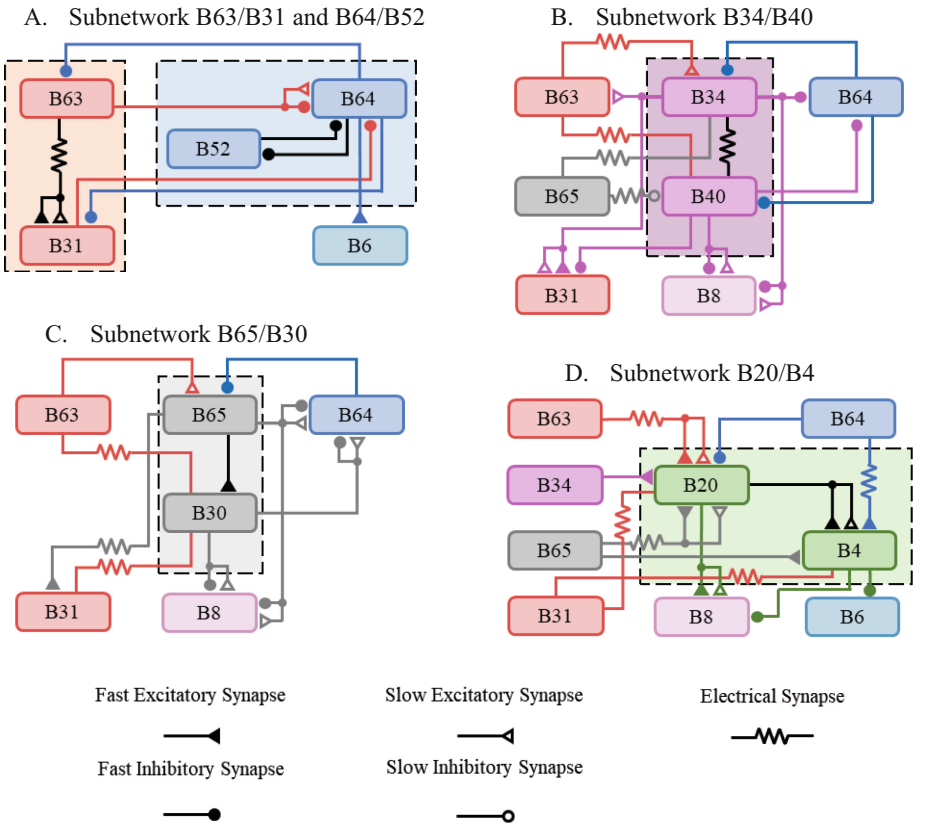

Fig. 2. Schematic of the buccal ganglion layer. This layer contains five subnetworks critical for multifunctional feeding control of *Aplysia.* A. Pathways of subnetworks B63/B31 and B64/B52. B. Pathways of subnetwork B34/B40. C. Pathways of subnetwork B65/B30. D. Pathways of B20/B4. Neurons in different subnetworks are highlighted in different colors, and each subnetwork is enclosed by a dashed and color-coded rectangle. The synaptic connections are color-coded according to their presynaptic neurons, with the exception that those within each subnetwork are black.

implications in terms of biting and swallowing. CBI-2 excites the B34/B40 subnetwork but inhibits B65 [17], leading to a longer protraction and biting-like pattern. CBI-4, by contrast, shortens the protraction phase by exciting B30 [16], making the pattern more like swallowing. The activations of CBIs are determined by the same feedback pathways in [2] so that they can coordinate behavioral switching based on exteroceptive stimuli.

2.4 Model Implementation

We implemented the neuromechanical model in the MATLAB Simulink/Multibody environment (R2021b). The parameters of the biomechanical model were taken from [2]. We referred to [7] to set the parameters governing the intrinsic dynamics of the neurons. We hand-tuned parameters to obtain realistic responses for those neurons that do not exist in [2] and for all chemical synapses. The simulation runs approximately two times faster than in real-time in accelerator mode on a 3.0 GHz CPU machine.

3 Results

3.1 Multifunctional Feeding Control

The model qualitatively generates multifunctional feeding behaviors of *Aplysia californica,* including biting, swallowing, and rejection (Fig. 3). Rhythmic biting patterns mediated by the SNS controller possess similar protraction duration and retraction duration, with weak grasper closure in-phase with retraction. As in the previously reported biomechanical model by Webster-Wood et al. [2], we neglect the interactions between the muscles and the environment during biting, so no force is experienced by the seaweed (Fig. 3A). The protraction duration is slightly shorter than the retraction duration during swallowing (Fig. 3B), as observed during swallowing behavior in the animal. A large positive (ingestive) force is exerted on the seaweed during retraction. The feedback pathways enable the model to adjust its retraction according to the external load, such that the period of high-load swallowing is longer than that of no-load biting (see below). The model can also successfully generate rejection-like behaviors (Fig. 3C). The period of rejection is much longer than ingestive patterns, and the force on the seaweed is negative (egestive) during the protraction phase, which is again similar to what is observed in the animal.

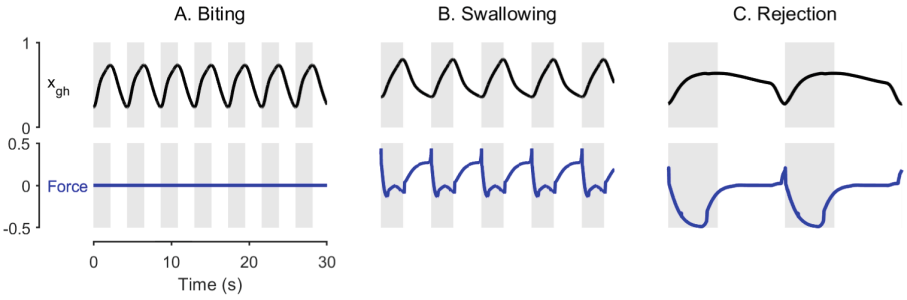

Fig. 3. The integration of the SNS model and simplified periphery is capable of producing kinematics (for biting) and both kinematics and kinetics (for swallowing and rejection) that are similar to those observed experimentally: A. Biting. B. Swallowing. C. Rejection. Shaded backgrounds indicate the protraction phase.

3.2 Comparison of Simulated Ingestive Behaviors with Animal Data

We quantitatively compared the model's behaviors to reported *Aplysia* experimental data (Fig. 4). The first data set is selected from [19] and compares ingestive motor pattern variability in intact animals (with sensory feedback) with variability in isolated ganglia (without sensory feedback) (Fig. 4A). *In vivo*, durations of biting are relatively short (4.26 $\pm$ 0.95 s), with similar mean values and variations (standard deviation) of the protraction phase (2.03 $\pm$ 0.62 s) and the retraction phase (2.17 $\pm$ 0.60 s). In contrast, the behavioral durations greatly increase when sensory feedback is removed (15.66 $\pm$ 7.34 s) (Fig. 4B). This increase in duration occurs mainly in protraction duration (10.40 $\pm$ 5.78 s), with a lesser increase in retraction duration (4.99 $\pm$ 3.28 s). The SNS model can generate similar biting behaviors with and without proprioceptive feedback (Fig. 4A, B). When the feedback signal of the grasper position (x_{gh}) is included, the duration of biting is 4.44 s. As in the animal data, the difference between the protraction duration (2.15 s) and the retraction duration (2.29 s) is minimal. When the proprioceptive feedback is removed in the model, the protraction duration significantly increases to 12.04 s, while the retraction duration (5.77 s) only experiences a moderate prolongation. The contrast between the durations with and without feedback illustrates the critical role proprioceptive pathways could play in normal biting behavior.

The second dataset from [20] compared the swallowing durations under different load conditions (Fig. 4C, D). When animals feed on unloaded seaweed (unloaded swallowing), the total cycle duration is 5.46 $\pm$ 0.76 s. When they attempt to ingest unbreakable seaweed (loaded swallowing), the addition of load slows down the behavior, increasing the total duration by about 30% (7.11 $\pm$ 0.9 s). In simulations, the unloaded condition can be implemented by removing the joint connecting the seaweed to the ground. When the joint is removed, the duration of swallowing generated by the model is 5.25 s, with a slightly shorter protraction duration (2.59 s) than the retraction duration (2.66 s) (Fig. 4C,

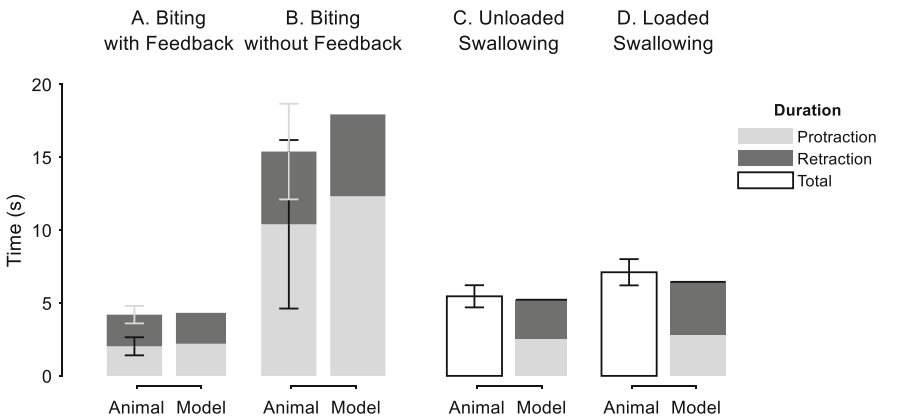

Fig. 4. Comparison of behavioral durations between the animal data and the model. The model was validated based on four experiments: A. *in vivo* biting [19]. B. Ingestive patterns generated by isolated ganglia [19]. C. Swallowing unloaded seaweed [20]. D. Swallowing unbreakable seaweed [20]. Error bars indicate standard deviations.

D). The restoration of the seaweed constraint increases the total duration by about 23% (6.45 s). Thus, the model data also follows the trend observed in the animal data that the increase of load results in longer ingestive durations.

4 Conclusions and Future Directions

We presented a Synthetic Nervous System that controls *Aplysia* feeding behaviors in simulation. The circuitry in the motor control layer and buccal ganglion layer is organized into nine subnetworks that generate activity patterns needed for biting, swallowing, and rejection. CBIs in the cerebral ganglion can coordinate feeding behaviors by modulating these subnetworks.

We then implemented the neural circuitry model in a simplified *Aplysia* biomechanical model. We found in simulations that this neuromechanical model is qualitatively sufficient to generate the three key feeding behaviors biting, swallowing, and rejection. Furthermore, by comparing the model's output with animal data, we demonstrated that the model produces similar outputs for *Aplysia* feeding behaviors under four different conditions (biting with feedback, biting without feedback, unloaded swallowing, loaded swallowing). Specifically, the integration of proprioceptive pathways considerably shortens the protraction phase during biting. Such variation in the protraction duration is due to the protraction-triggered excitatory feedback to B64 considered in our model. When the protraction of the grasper is strong enough (x_{gh} higher than a threshold), it tends to excite B64. The strength of the feedback is proportional to the difference between x_{gh} and the threshold in our model. Thus, incorporating it accelerates the termination of the protraction phase. If the feedback pathways are removed, the earlier onset of B64 also disappears. The intrinsic pattern generator will then produce a biting pattern featured with a long protraction phase. The feedback pathways influencing the termination of the B64 firing also exist in our model (retraction-triggered inhibitory feedback), indicating that a strong retraction of the grasper (x_{gh} lower than a threshold) tends to inhibit B64 and accelerates the termination of the retraction phase. However, the threshold of the pathways is set relatively low so that x_{gh} will not become much lower than the threshold before the termination of the retraction phase, while it can become much higher than the threshold before the termination of the protraction phase. Therefore, the retraction-triggered inhibitory feedback is generally weaker than protraction-triggered excitatory feedback in our model, and the variation in the retraction duration with and without feedback is less obvious than in the protraction phase. These results highlight the role of proprioceptive feedback in coordinating movements, and they suggest experimentally testable pathways by which robust responses to load are produced in the animal.

To further verify the predictive ability of the proposed model, we will compare its response with more animal data at both neural and behavioral levels. According to these results, we can tune the unknown parameters and determine whether it is necessary to include additional identified neurons and synaptic connections in the model. A good neural circuitry model should also generate robust control with uncertainties in the model parameters. Performing sensitivity analysis is critical to evaluate how much the variation in certain parameters will contribute to the variation in the model output.

Because the proposed computational model is rooted in neurobiology, it could serve as a guide in the experimental study of *Aplysia* feeding or as a platform for hypothesis testing. Furthermore, it is also possible to generalize the model for robotic control because the single-compartment and non-spiking neuron models in the SNS reduce the computational complexity and allows real-time implementation.

Acknowledgements. This work was supported by NSF DBI 2015317 as part of the NSF/CIHR/DFG/FRQ/UKRI-MRC Next Generation Networks for Neuroscience Program and NSF IIS1704436.

References

1. Chen, J.: Food oral processing - a review. Food Hydrocolloid. **23**(1), 1–25 (2009). https://doi.org/10.1016/j.foodhyd.2007.11.013
2. Webster-Wood, V.A., Gill, J.P., Thomas, P.J., Chiel, H.J.: Control for multifunctionality: bioinspired control based on feeding in *Aplysia californica*. Biol. Cybern. **114**(6), 557–588 (2020). https://doi.org/10.1007/s00422-020-00851-9
3. Huan, Y., et al.: Carbon fiber electrodes for intracellular recording and stimulation. J Neural Eng. **18**(6), 1–18 (2021). https://doi.org/10.1088/1741-2552/ac3dd7
4. Wolpert, D.M., Ghahramani, Z.: Computational principles of movement neuroscience. Nat Neurosci. **3**, 1212–1217 (2000). https://doi.org/10.1038/81497
5. Mangan, E.V., Kingsley, D.A., Quinn, R.D., Sutton, G.P., Mansour, J.M., Chiel, H.J.: A biologically inspired gripping device. Industrial Robot Int J. **32**, 49–54 (2005). https://doi.org/10.1108/01439910510573291
6. Cataldo, E., Byrne, J.H., Baxter, D.A.: Computational Model of a Central Pattern Generator. In: Priami, C. (ed.) CMSB 2006. LNCS, vol. 4210, pp. 242–256. Springer, Heidelberg (2006). https://doi.org/10.1007/11885191_17
7. Costa, R.M., Baxter, D.A., Byrne, J.H.: Computational model of the distributed representation of operant reward memory: combinatoric engagement of intrinsic and synaptic plasticity mechanisms. Learn Memory. **27**(6), 236–249 (2020). https://doi.org/10.1101/lm.051367.120
8. Szczecinski, N.S., Hunt, A.J., Quinn, R.D.: A functional subnetwork approach to designing synthetic nervous systems that control legged robot locomotion. Front Neurorobotics. **11**, 1–19 (2017). https://doi.org/10.3389/fnbot.2017.00037
9. Hurwitz, I., Neustadter, D., Morton, D.W., Chiel, H.J., Susswein, A.J.: Activity patterns of the B31/B32 pattern initiators innervating the I2 muscle of the buccal mass during normal feeding movements in *Aplysia californica*. J Neurophysiol. **75**(4), 1309–1326 (1996). https://doi.org/10.1152/jn.1996.75.4.1309
10. Morton, D.W., Chiel, H.J.: *In vivo* buccal nerve activity that distinguishes ingestion from rejection can be used to predict behavioral transitions in *Aplysia*. J Comp Physiology. **172**(1), 17–32 (1993). https://doi.org/10.1007/bf00214712
11. McManus, J.M., Lu, H., Cullins, M.J., Chiel, H.J.: Differential activation of an identified motor neuron and neuromodulation provide *Aplysia*'s retractor muscle an additional function. J Neurophysiol. **112**(4), 778–791 (2014). https://doi.org/10.1152/jn.00148.2014
12. Sutton, G.P., et al.: Passive hinge forces in the feeding apparatus of *Aplysia* aid retraction during biting but not during swallowing. J Comp Physiology. **190**(6), 501–514 (2004). https://doi.org/10.1007/s00359-004-0517-4
13. Hurwitz, I., Ophir, A., Korngreen, A., Koester, J., Susswein, A.J.: Currents contributing to decision making in neurons B31/B32 of *Aplysia*. J Neurophysiol. **99**(2), 814–830 (2008). https://doi.org/10.1152/jn.00972.2007

14. Hurwitz, I., Kupfermann, I., Susswein, A.J.: Different roles of neurons B63 and B34 that are active during the protraction phase of buccal motor programs in *Aplysia californica*. J Neurophysiol. **78**(3), 1305–1319 (1997). https://doi.org/10.1152/jn.1997.78.3.1305
15. Elliott, C.J.H., Susswein, A.J.: Comparative neuroethology of feeding control in molluscs. J Exp Biology. **205**, 877–896 (2002). https://doi.org/10.1242/jeb.205.7.877
16. Jing, J., Cropper, E.C., Hurwitz, I., Weiss, K.R.: The construction of movement with behavior-specific and behavior-independent modules. J Neurosci. **24**(28), 6315–6325 (2004). https://doi.org/10.1523/jneurosci.0965-04.2004
17. Jing, J., Weiss, K.R.: Generation of variants of a motor Act in a modular and hierarchical motor network. Curr Biol. **15**(19), 1712–1721 (2005). https://doi.org/10.1016/j.cub.2005.08.051
18. Jing, J., Weiss, K.R.: Neural mechanisms of motor program switching in *Aplysia*. J Neurosci. **21**(18), 7349–7362 (2001). https://doi.org/10.1523/jneurosci.21-18-07349.2001
19. Cullins, M.J., Gill, J.P., McManus, J.M., Lu, H., Shaw, K.M., Chiel, H.J.: Sensory feedback reduces individuality by increasing variability within subjects. Curr Biol. **25**(20), 2672–2676 (2015). https://doi.org/10.1016/j.cub.2015.08.044
20. Gill, J.P., Chiel, H.J.: Rapid Adaptation to Changing Mechanical Load by Ordered Recruitment of Identified Motor Neurons. ENEURO.0016-20.2020. 7(3), 1–18 (2020). https://doi.org/10.1523/eneuro.0016-20.2020